


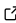
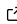
1 FELINE: A tool to detect emission line galaxies in 3d 2 data

3 Martin Wendt ^{*1}, Marvin Henschel ², and Oskar Fjonn Soth ²

4 ¹ Institute of Physics and Astronomy, University of Potsdam, 14476 Potsdam, Germany ² Institute of
5 Computer Science and Computational Science, University of Potsdam, 14476 Potsdam, Germany

DOI: [10.xxxxxx/draft](https://doi.org/10.xxxxxx/draft)

Software

- [Review](#) 
- [Repository](#) 
- [Archive](#) 

Editor: 

Submitted: 12 September 2024

Published: unpublished

License

Authors of papers retain copyright
and release the work under a
Creative Commons Attribution 4.0
International License ([CC BY 4.0](#)).

In partnership with



AMERICAN
ASTRONOMICAL
SOCIETY

This article and software are linked
with research article DOI
[10.3847/xxxxx](https://doi.org/10.3847/xxxxx) <- [update this](#)
[with the DOI from AAS once you](#)
[know it.](#), published in the
Astrophysical Journal <- The
name of the AAS journal..

6 Summary

7 The detection and classification of objects in astrophysical data has been a key task since
8 the earliest days of astronomy. Over the past decade, the volume of newly observed data has
9 increased dramatically. The advent of integral field unit spectrographs (IFUs), which produce
10 3D data cubes, has shifted the focus from classical single-target observations to much broader
11 fields of view captured in a single exposure. Simple flux-level peak detection algorithms based
12 on thresholding are prone to either missing many potential real objects or, as a trade-off,
13 producing an abundance of false positives.

14 The VLT/MUSE ([R. Bacon et al., 2010, 2014](#)) 3D spectrograph creates $\sim 90,000$ medium
15 resolution spectra arranged in a 300×300 spatial grid. These data cubes have typical sizes of
16 3–6 GiB per exposure, the sheer amount of data asks for automated processes to support the
17 scientists.

18 The *Find Emission LINEs* tool FELINE combines a fully parallelized galaxy line template
19 matching with the matched filter approach for individual emission features of LSDcat ([Herenz,](#)
20 [2023](#); [Herenz & Wisotzki, 2017](#)). The FELINE algorithm evaluates the likelihood of emission
21 lines at specific positions in each spectrum of the data cube. It does this by probing all possible
22 combinations of up to 14 typical emission features, including H α , H β , H γ , H δ , [OII], [OIII],
23 [NII], [SII], and [NeIII], for the redshift range of interest ($0.4 < z < 1.4$). This extensive
24 analysis leads to approximately 230,400,000,000 iterations.

25 Science field

26 The signal-to-noise cube generated after matched filtering with a 3D emission line template
27 reflects the probability of an emission line at a given spatial and spectral position. This
28 probability is significantly boosted by the filtering process. As a result, galaxies with multiple
29 weak emission features can be detected with a significance that substantially exceeds the
30 significance of each individual contributing line. This approach is particularly successful for
31 galaxies that show no or little continuum flux in the data, and therefore would generally go
32 undetected in imaging data alone.

33 FELINE was used for the galaxy catalogs of the MEGAFLOW survey in ([Cherrey et al., 2024](#);
34 [Langan et al., 2023](#); [Schroetter et al., 2024](#)).

35 Implementation

36 The tool uses a brute-force search through the parameter space. Due to the size of the
37 parameter space, the language of implementation was chosen as C for computational efficiency.

*mwendt@astro.physik.uni-potsdam.de

38 This approach demonstrates the success of filtering the data with expected templates for
39 individual emission lines, rather than testing full physical models of galaxies (including simulated
40 continuum and temperature-broadened emission lines) against the raw observed data. This
41 reduces the individual models to a single position at which the likelihood of a line is being
42 probed.

43 For each set of parameters (spatial position in the cube, redshift, and line composition),
44 the FELINE algorithm returns the value of the highest-scoring combination, along with its
45 corresponding redshift and line composition.

46 The data cube contains 300×300 spectra, each of which is relatively small ($< 64\text{KB}$). The
47 algorithm performs 512×5000 iterations on each spectrum, returning only 3 values: the quality
48 of the best match, the redshift of the best match, and the line combination of the best match.
49 Importantly, the outer 300×300 iterations are completely independent of each other.

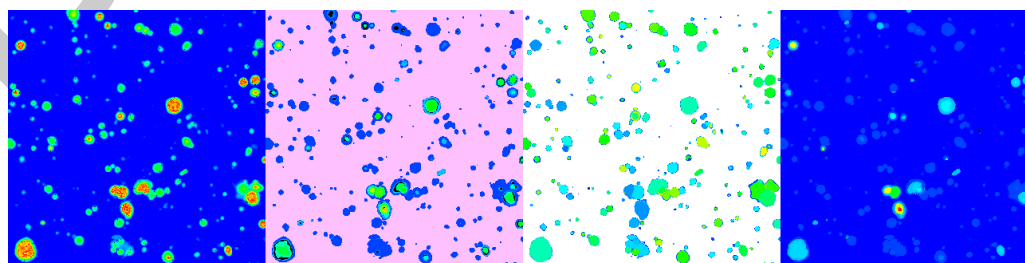
50 To take advantage of this independence, the code utilizes full parallelization of the outer loop
51 using OpenMP, with most variables shared due to their independence. As a result, FELINE
52 scales quite well with the number of CPU cores. Runtimes for the FELINE code on the provided
53 2.8 GB example cube (Roland Bacon et al., 2023) (CC BY-NC-SA 4.0):

Device	Cores	Runtime in seconds
AMD_EPYC_7542	1	1150
AMD_EPYC_7542	4	282
AMD_EPYC_7542	8	141
AMD_EPYC_7542	16	71
NVIDIA A100 GPU	64	27

54 Another major improvement in execution time was accomplished by re-arranging the data to
55 maximize the amount of cache hits. Initially, the cube data is stored as a series of images,
56 i.e., 300×300 spatial data points arranged in an array of 4,000 in spectral dimension. The
57 algorithm works on spectral which would be strongly interleaved by ~ 360 KB for consecutive
58 data points and the full spectrum exceeding a range of 1 GiB. As a preprocessing step, the
59 data cube is re-arranged as a spatial grid of full spectra.

60 That arrangement further motivated an implementation of FELINE in CUDA to utilize GPUs for
61 parallelization. Typical full size MUSE data cubes can be fully loaded into the GPU memory of
62 any modern CUDA capable GPU. We provide a working implementation that produces identical
63 results to the FELINE C variant.

64 Optionally, FELINE plots the three return parameters in real time via SDL surface along with
65 storing them on disk.



66 Shown are from left to right the quality of the best match, the corresponding redshift of the
67 best match and its template. A fourth panel shows the number of lines that contributed to
68 the most successful model for ease of human readability (it reflects the number of set bits in
69 the best model value).
70

71 We provide a python framework to further visualize and verify the FELINE detections.

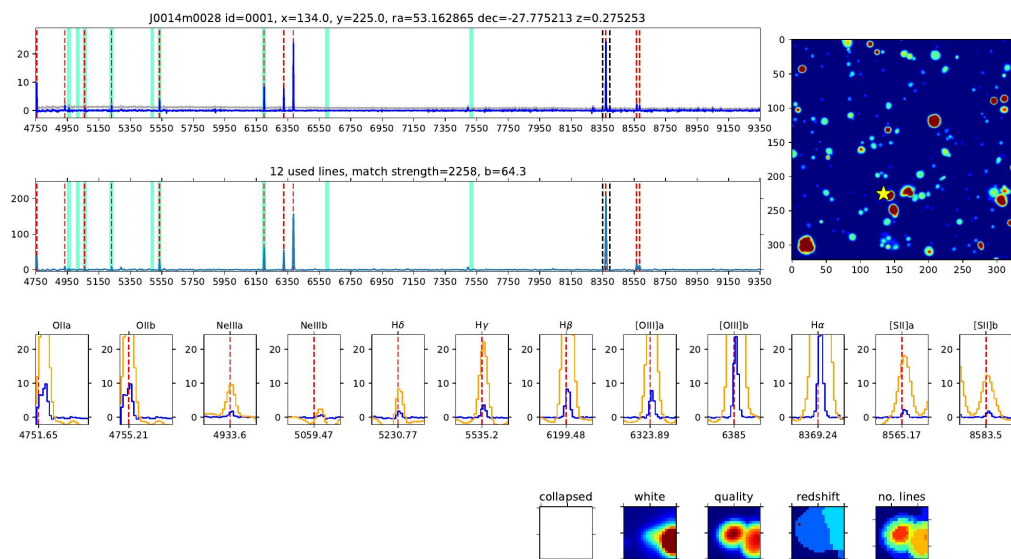


Figure 1: Plot generated from the FELINE result.

72 Acknowledgements

73 We acknowledge the work on LSDcat by Christian Herenz

74 References

- 75 Bacon, R., Accardo, M., Adjali, L., Anwand, H., Bauer, S., Biswas, I., Blaizot, J., Boudon, D.,
76 Brau-Nogue, S., & Brinchmann. (2010). The MUSE second-generation VLT instrument.
77 In I. S. McLean, S. K. Ramsay, & H. Takami (Eds.), *Ground-based and airborne instru-*
78 *mentation for astronomy III* (Vol. 7735, p. 773508). <https://doi.org/10.1117/12.856027>
- 79 Bacon, Roland, Brinchmann, J., Conseil, S., Maseda, M., Nanayakkara, T., Wendt, M., Bacher,
80 R., Mary, D., Weilbacher, P. M., Krajnović, D., Boogaard, L., Bouché, N., Contini, T.,
81 Epinat, B., Feltre, A., Guo, Y., Herenz, C., Kollatschny, W., Kusakabe, H., ... Zoutendijk,
82 S. L. (2023). The MUSE Hubble Ultra Deep Field surveys: Data release II. *670*, A4.
83 <https://doi.org/10.1051/0004-6361/202244187>
- 84 Bacon, R., Vernet, J., Borisova, E., Bouché, N., Brinchmann, J., Carollo, M., Carton, D.,
85 Caruana, J., Cerda, S., Contini, T., Franx, M., Girard, M., Guerou, A., Haddad, N., Hau,
86 G., Herenz, C., Herrera, J. C., Husemann, B., Husser, T.-O., ... Zins, G. (2014). MUSE
87 Commissioning. *The Messenger*, *157*, 13–16.
- 88 Cherrey, M., Bouché, N. F., Zabl, J., Schroetter, I., Wendt, M., Langan, I., Richard, J.,
89 Schaye, J., Mercier, W., Epinat, B., & Contini, T. (2024). MusE GAS FLOW and Wind
90 (MEGAFLOW) X. The cool gas and covering fraction of Mg II in galaxy groups. *528*(1),
91 481–498. <https://doi.org/10.1093/mnras/stad3764>
- 92 Herenz, E. C. (2023). Revisiting the emission line source detection problem in integral field
93 spectroscopic data. *Astronomische Nachrichten*, *344*(5), e20220091. <https://doi.org/10.1002/asna.20220091>
- 94
- 95 Herenz, E. C., & Wisotzki, L. (2017). LSDCat: Detection and cataloguing of emission-line
96 sources in integral-field spectroscopy datacubes. *602*, A111. <https://doi.org/10.1051/0004-6361/201629507>
- 97
- 98 Langan, I., Zabl, J., Bouché, N. F., Ginolfi, M., Popping, G., Schroetter, I., Wendt, M., Schaye,

- 99 J., Boogaard, L., Freundlich, J., Richard, J., Matthee, J., Mercier, W., Contini, T., Guo,
100 Y., & Cherrey, M. (2023). MusE GAs FLOW and Wind (MEGAFLOW) IX. The impact of
101 gas flows on the relations between the mass, star formation rate, and metallicity of galaxies.
102 521(1), 546–557. <https://doi.org/10.1093/mnras/stad357>
- 103 Schroetter, I., Bouché, N. F., Zabl, J., Wendt, M., Cherrey, M., Langan, I., Schaye, J., & Contini,
104 T. (2024). MusE GAs FLOW and Wind (MEGAFLOW). XI. Scaling relations between
105 outflows and host galaxy properties. 687, A39. [https://doi.org/10.1051/0004-6361/
106 202348725](https://doi.org/10.1051/0004-6361/202348725)

DRAFT